ARMA 17-MTS lecture

Vertical stress profiles and long-term rock mass rheology

Cornet, F.H.
EOST-Univ. de Strasbourg, France

This paper was prepared for presentation at the 51st US Rock Mechanics / Geomechanics Symposium held in San Francisco, California, USA, 25-28 June 2017. This paper was selected for presentation at the symposium by an ARMA Technical Program Committee based on a technical and critical review of the paper by a minimum of two technical reviewers. The material, as presented, does not necessarily reflect any position of ARMA, its officers, or members. Electronic reproduction, distribution, or storage of any part of this paper for commercial purposes without the written consent of ARMA is prohibited. Permission to reproduce in print is restricted to an abstract of not more than 200 words; illustrations may not be copied. The abstract must contain conspicuous acknowledgement of where and by whom the paper was presented.

ABSTRACT: Borehole imaging logs together with hydraulic tests in boreholes provide very efficient means for determining in situ the complete stress tensor at various depths. When combined with focal mechanisms of induced seismicity, these data may be used to map spatial variations of pore pressure.
The discussion of such a vertical stress profile, as obtained in the French Paris Basin sedimentary formations, helps us outline the importance of visco-elasticity on stress. In particular it demonstrates the role of pressure-solution and climatic variations on the local present-day stress field. This has strong consequences for a better understanding of intraplate seismicity.

1. INTRODUCTION: THE REGIONAL SESS FIELD AND ITS SOURCE

For many a rock engineering project, the regional stress field is an essential boundary condition. At a point, the stress is defined by a symmetrical tensor with six independent components so that, at any given time, the regional stress field is described by six functions of time and of the three spatial coordinates.

We review first various approaches that help produce these six functions, when time variations are neglected. This process is illustrated by two examples: one taken in a granite massif and one taken from the French Paris Basin sedimentary formations. The location is that of the underground laboratory developed for investigating the characteristics of a long term radioactive waste repository.

We show the limits of elastic modelling for identifying the sources of this stress field and consider the effect of gravity on an orthotropic visco-elastic formation. The time dependency is linked to pressure solution and climatic variations.

This helps us propose a new paradigm for analyzing the regional stress field in intraplate regions where no tectonic activity is presently identified.

2. REGIONAL STRESS FIELD EVALUATIONS

In a geographical frame of reference, it is very often convenient to characterize the stress tensor by the three angles that define the local principal stress directions and by the three principal stress components.

When topography effects may be neglected, one principal component of the regional stress field may be assumed a priori to be vertical (noted σ_v). The two other components are horizontal and noted respectively σ_H and σ_h for the maximum and the minimum horizontal components.

The world stress map (Zoback, 1992, Heidbach et al., 2010) proposes a compilation of all stress field evaluations that have been conducted in the world. Results are plotted on the assumption that one principal component is vertical. This catalog (the 2016 release is available at *www.world-stress-map.org/*) should always be consulted before undertaking a local evaluation. It may help obtain useful information on the regional principal stress directions.

But stress vary with depth and for most engineering projects some precise evaluation of these variations is necessary. This information may be derived from borehole investigations as well as from natural or induced micro-seismic analysis.

2.1. *Geophysical borehole investigations for principal stress directions identification*

Geophysical investigations include borehole wall imaging (ultrasonic or electrical techniques) as well as P and S wave velocity azimuthal variations as determined from specialized sonic logs.

Because boreholes perturb locally the regional stress field, identification of these perturbations may be taken to advantage for identifying principal stress directions. Indeed, when the borehole is parallel to a principal stress direction, the tangential component is maximum in the direction parallel to that of the minimum principal stress perpendicular to the borehole axis. It is minimum in the direction parallel to that of the maximum principal stress component normal to the borehole axis (e.g. Cornet [chapt.5], 2015, Zoback [chapt. 6], 2010).

For azimuths where compression failure conditions are satisfied, some breakouts develop and their mapping help identify the orientation of the minimum principal component orientation.

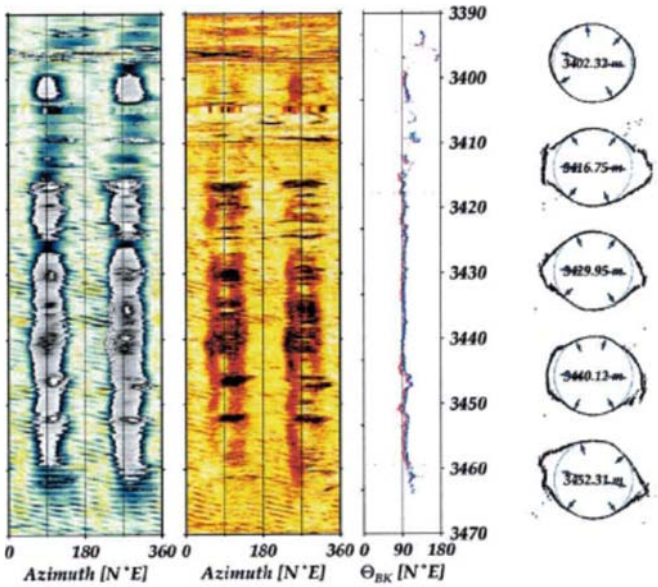

Fig. 1. Example of borehole breakouts in Granite as mapped by ultrasonic imaging (Berard and Cornet, 2003)

Similarly, in location where the minimum tangential stress components has satisfied tensile failure conditions, tensile fractures develop and their mapping yields the orientation of the maximum principal stress in the direction normal to the borehole axis.

When no failure develops, principal stress directions may still be identified by investigating azimuthal variations in seismic velocity as identified with dipole sonic logs (Lei et al., 2012). Dipole sonic logs generate both P and S waves that propagate along the borehole axis. Because rocks contain always some micro-cracks, they exhibit a non-linear elastic response. Hence detection of directions for which seismic velocities reach extremum values help identify far-field principal stress directions.

Because these logs cover long borehole lengths, they provide a unique evaluation of the stress field continuity. They also help identify main zones of heterogeneity. This information is essential for locating properly zones selected for local hydraulic testing.

2.2. *Borehole hydraulic testing for a complete principal stress components evaluation*

- **The Classical Hydraulic Fracturing technique**

A fracture-free portion in a borehole, parallel to a principal stress direction, is isolated with an inflatable straddle packer (example of packer pressure given by the top blue curve in figure 2).

The isolated interval is then pressurized with a constant flow rate (lower part of fig.2) till a fracture occurs. After the hydraulic fracture has been propagated for a short distance, injection stops and the drop in pressure is recorded (green curve, step 1, in figure 2).

Then, after dropping the interval pressure to an arbitrary low value, injection is restarted at constant flow rate and the fracture is propagated on a distance equal to four or five borehole diameters. Injection stops and the drop in pressure is recorded (green curve, step 2, in fig. 2).).

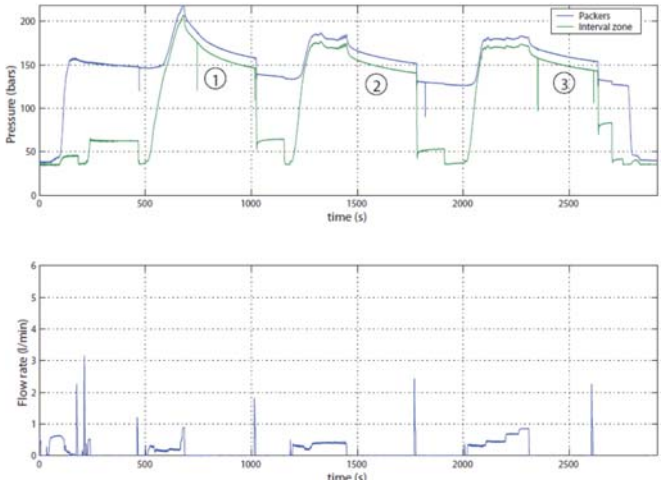

Fig.2 Pressure and flow rate records for a classical hydraulic fracturing test (Cornet [chapt. 13], 2015)

During step 3, the fracture is reopened with an injection flow rate increased step by step. When the flow rate increase does not alter significantly the interval pressure, injections stops and the drop in interval pressure is recorded.

Detailed analysis of the pressure drop observed during step 2 yields the so called shut-in pressure (Haimson and Cornet, 2003). Analysis of the flow rate – pressure record observed during step 3 yields the quasi-static reopening pressure. The mean value between step 2 shut-in pressure and step 3 quasi-static reopening pressure may be considered a sound estimate of the far field

minimum principal stress magnitude (Cornet et al., 2003). Comparison of this value with the step 1 shut-in pressure and the step 3 shut in pressure may be taken to advantage for discussing the fracture growth.

The surge in pressure observed at the end of each step, after the interval pressure has been dropped suddenly, is caused by some fluid flow back to the packed off interval (fig. 2). It constitutes a useful test of the testing system tightness and provides a demonstration that the fracture has not extended axially beyond the packers.

The peak of interval pressure observed in step 1 (fig. 2) is called the breakdown pressure and is used often for determining the magnitude of the maximum principal stress component normal to the borehole axis. But, personally, I discourage this practice for the following four reasons:

- ✓ In many cases, electrical images obtained just after testing have demonstrated that the fracture extends some distance along the packers and that most likely it has been initiated by the packers;
- ✓ When the stiffness of the testing system is not high enough, the fracture initiates sometime before the interval pressure reaches its peak. In fact fracture occurs when the pressure- time curve gets non-linear (Ito et al., 1999).
- ✓ Permeability depends strongly on stress and therefore its characteristics vary with azimuth at the borehole wall. This creates difficulty for taking into account properly effects of pore pressure.
- ✓ Finally, the mechanics of fracture initiation involves the growth of micro-cracks the characteristics of which are generally unknown.

This introduces too many unknowns that hampers the reliability of such evaluations and alternative methods have been developed.

- **Hydraulic testing of preexisting fractures**

Laboratory experiments on hydraulic fracturing has shown that, when pre-existing fractures exist in the packed off interval, these fractures may, or may not, influence the formation of a new fracture, depending on flow rate (Cornet and Valette, 1984). This observation is taken to advantage with the hydraulic testing of pre-existing fractures (HTPF) method (Cornet, 1993).

The section of a borehole, where only one preexisting fracture has been identified, is packed off with an inflatable straddle packer. The interval pressure is raised progressively, step by step, till the interval pressure-flow rate record changes slope significantly. When the injection flow rate stops, the subsequent interval pressure drop is monitored. Analysis of the pressure drop yields an estimate of the shut-in pressure, which is taken equal to the normal stress, $\sigma_n(\underline{N})$, supported by the fracture with normal $\underline{N}$ away from the well:

$$\sigma_n(\underline{N}) = \sigma_{ij}\, N_i\, N_j, \qquad (1)$$

σ_{ij}, Ni, Nj are respectively the components of the far-field stress tensor (assumed to be uniform) and of the unit normal to the tested fracture, as expressed in the ($\mathbf{I_1}$, $\mathbf{I_2}$, $\mathbf{I_3}$) frame of reference.

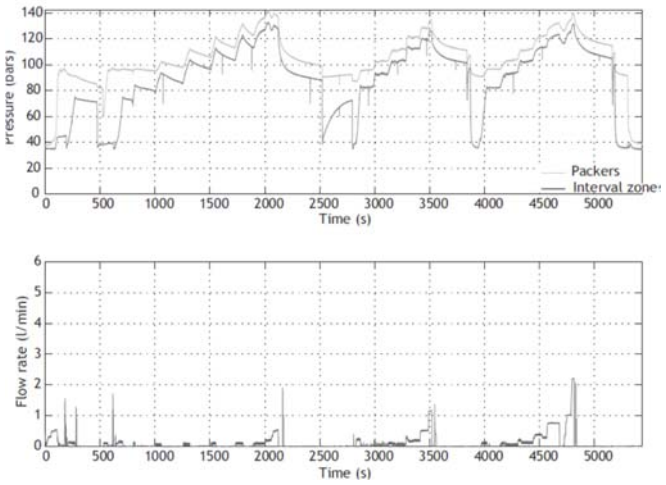

Figure 3. Pressure and flow rate records for an HTPF test.

σ_{ij} corresponds to six unknowns, whilst one HTPF test yields only one data point, $\sigma_n(\underline{N})$, given the components of the unit normal to the fracture plane are derived from geophysical logs.

When HTPF tests are too distant from one another, the stress field is not constant over the whole tested volume and it is assumed to vary linearly with spatial coordinates. Hence equation (1) involves 24 unknown. But equilibrium conditions provide another 3 equations with one additional unknown (the rock mass density) so that the system of equations to be solved involves 22 unknowns.

The linear spatial stress variation approximation is often well adapted to crystalline rocks. Further these formations exhibit frequently a large range of orientations of preexisting fractures.

But the linear approximation cannot be applied in sedimentary formations in which the stress field vary non-linearly from bed to bed (see section 3). In such formations, HTPF has revealed of great help for measuring the vertical stress component from tests on preexisting horizontal joints (see section 3).

- **Hydraulic fracturing in inclined wells**

When the pressurized section of the well is inclined to all principal stress directions, the radial component ($\sigma_{\rho\rho}$) of the stress tensor at the borehole wall is a principal component (σ_ρ), which is equal to the applied pressure ($\sigma_\rho = P_w$). Here we reckon compression as being

positive. The three other components are (e.g. Cornet [chapt.12], 2015)

$$\sigma_{\theta\theta} = \sigma_{11} + \sigma_{22} - 4[(\sigma_{11} - \sigma_{22}) \cos 2\theta)/2 + \sigma_{12} \sin 2\theta] - P_w \quad (2)$$

$$\sigma_{zz} = \sigma_{33} - 4\nu [(\sigma_{11} - \sigma_{22}) \cos 2\theta)/2 + \sigma_{12} \sin 2\theta] \quad (3)$$

$$\sigma_{\theta z} = 2 (\sigma_{23} \cos\theta - \sigma_{31} \sin \theta) \quad (4)$$

The two principal components that depend on the azimuthal coordinate θ, at the borehole wall, are respectively

$$\sigma_M = 1/2 (\sigma_{\theta\theta} + \sigma_{zz}) + [(\sigma_{\theta\theta} - \sigma_{zz})^2 + 4 \sigma_{\theta z}^2]^{1/2} \quad (5)$$

$$\sigma_m = 1/2 (\sigma_{\theta\theta} + \sigma_{zz}) - [(\sigma_{\theta\theta} - \sigma_{zz})^2 + 4 \sigma_{\theta z}^2]^{1/2} \quad (6)$$

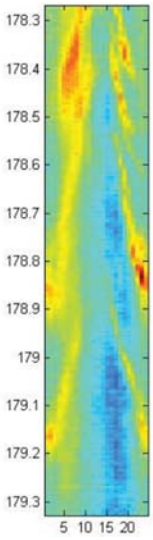

Fig. 4. Electrical image of *en échelon* fractures generated by hydraulic fracturing in a well inclined by more than 20° to any principal stress direction. The dip and azimuth of the fractures depend on all the far-field stress components. This is taken to advantage for evaluating the maximum horizontal principal stress magnitude when all other stress components are known (Cornet [chapt. 12], 2015).

When pressure P_w in the well is increased, the minimum principal stress σ_m gets progressively negative till a hydraulic fracture is created normal to the local minimum principal stress component. This occurs for two symmetrical azimuths so that the fracture plane is inclined to the borehole axis. This often generates a set of parallel inclined hydraulic fractures called *en échelon* fractures (see figure 4).

The azimuth θ of the fractures depends on all the far field stress components and is such that the partial derivative of σ_m with respect to θ, $\sigma_{m,\theta}$, is nul. When all the far field stress components but the maximum horizontal principal component, σ_H, are known, the measurement of the azimuth of *en echelon* fractures yields a first equation for computing, σ_H (Peska and Zoback, 1995). Another equation may be written by observing that these fractures do not support any shear stress. Hence the geometry of *en échelon* fractures yield two equations for one unknown and this ends up the complete stress determination.

2.3. Validation of the stress field characterization

- **Integration of results from geophysical logs and hydraulic tests**

Geophysical logs provide a tool for evaluating the validity of the continuity hypothesis inherent to a reliable regional stress field characterization. They help identify zones of main stress heterogeneity.

Each of the hydraulic tests provides results the uncertainty on which is assumed to be characterized by a normal distribution. Hence they are described by an expected value and the associated standard deviation. A given measurement is considered to be homogenous with the proposed stress field characterization when its expected value rests within plus or minus two standard deviations from the predicted value (90% confidence level).

When more than 30 % of the results are heterogeneous with respect to a proposed stress field characterization, validity of this characterization should be seriously questioned.

- **Integration with focal mechanisms of induced seismicity**

Another means for ascertaining the validity of a stress field evaluation is provided by integration with data of different origins.

Such is the case when some local micro-seismic activity has been monitored so that some local focal mechanisms have been determined.

Micro-seismic sources are assumed to correspond to double couples characterized by their two nodal planes (see e.g. Cornet [chapt. 12], 2015). One of the nodal planes is the shear plane and the normal to the other nodal plane yields the direction of slip in the shear plane. Assuming this unit vector is parallel to the shear stress component supported by the plane before seismic slip occurs, its orientation helps constraining four components of the local stress tensor: the three Euler angles that define the principal stress direction and a factor R that characterizes the ellipticity of the tensor:

$$R = (\sigma_2 - \sigma_1)/ (\sigma_3 - \sigma_1) \quad (7)$$

where $\sigma_1, \sigma_2, \sigma_3$ are the principal stress components with $\sigma_3 \leq \sigma_2 \leq \sigma_1$ (Gephart and Forsyth, 1984, Maury et al., 2013).

When the induced micro-seismicity results from large water injections in wells where hydraulic tests have been conducted, all results may be integrated for a common stress field evaluation.

This has been the case for example for the 1,000 m deep granite test site at Le Mayet de Montagne, France (Yin and Cornet, 1994). On site some 22 HF and HTPF tests have been conducted in two vertical wells distant some 100 m from one another. A total of 87 focal mechanisms

have been determined within a volume equal to about $15x10^6$ m^3. A continuous stress field varying linearly with depth has been found to be compatible with 21 hydraulic tests (95% of the tests) but only 70% of the focal mechanisms.

It has been concluded that a regional stress field may be defined for this site. But 30% of the induced micro-seismic events occur in fractures that are heterogeneous to this stress field. For those 70% that are consistent, identification of the slip plane provides means to determine the local pore pressure given the local stress is known and assuming an effective stress Coulomb slip criteria (Cornet and Yin, 1995). This mapping of the far field pore pressure variation associated with the various water injections has helped constrain the understanding of this granite rock mass hydro-mechanical behavior.

3. A COMPLETE STRESS PROFILE IN THE SEDIMENTARY PARIS BASIN (FRANCE)

ANDRA, the French agency in charge of developing a safe underground nuclear waste repository, is investigating the potential of the Callovo-Oxfordian argillite (mudstone) formation in the Paris Basin. This 200 m thick layer is interbedded between two, several hundred netters thick, carbonate units, namely the Dogger and the Oxfordian limestones.

An underground laboratory has been developed at a depth of about 500 m, near the small village of Bure, after an extensive regional stress field determination program has been conducted in various vertical and inclined boreholes (Fig. 5, Wileveau et al. 2007; Cornet and Roeckel, 2012).

3.1. Borehole breakout analysis

Borehole breakouts have been observed in the Callovo-Oxfordian argillite in all borehole drilled with water based mud. But none were observed when oil based mud was used for drilling. This clearly demonstrates the role of mud chemistry on the arigilite mechanical behavior.

As a consequence only borehole breakouts orientations have been taken into account for the stress determination. The absence of breakouts in wells drilled with oil based mud has provided means to define an upper bound to the maximum horizontal principal stress magnitude in the argillite.

3.2. Hydraulic tests in vertical wells

Various true hydraulic fractures have been conducted in vertical sections of the wells. They helped constrain the minimum horizontal principal stress (magnitude and direction). For tests run with a stiff testing system, the breakdown pressure helped define an upper and a lower bound to the magnitude of the maximum horizontal principal stress depending on hypothesis on pore pressure effect.

Shut-in pressure values from a few HTPF tests run on horizontal joints provided the magnitude of the vertical stress component.

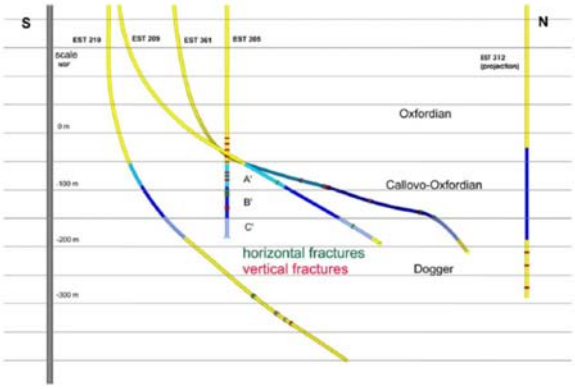

Fig. 5. Geometry of the various wells in which stress measurements have been conducted at Bure (depths are defined with respect to sea level) (Wileveau et al., 2007).

3.3. Hydraulic tests in inclined wells

Five of the six stress tensor components were known before running tests in the Dogger limestone. Hence the geometry of *en échelon* fractures observed in the inclined section of the well helped determine the magnitude of the maximum horizontal principal stress in this formation.

Results of the complete stress determination are shown on figure 6.

3.4. Pore pressure profile through direct in situ measurements

After the underground laboratory has been completed, detailed pore pressure measurements have been conducted in the argillite, as well as in the Dogger and the Oxfordian limestones (Fig. 7; Delay et al., 2007).

Permeability for the argillite has been measured in the 10^{-19} – 10^{-20} m^2 range. Interestingly, the pore pressure in the Oxfordian limestone is hydrostatic but that in the Dogger limestone is lower than hydrostatic. This demonstrates that the Callovo-Oxfordian argillite layer is an efficient barrier to downward flow.

In addition, a parabolic profile has been identified in the argillite but its origin is yet to be proposed. Indeed, as shown by Gonçalves et al. (2004), the osmotic hypothesis that has been proposed yields much too low values.

4. AN ORTHOTROPIC VISCO-PORO-ELASTIC MODEL

4.1. Limits of elastic models

In the Paris Basin, orientations of borehole breakouts as well as that of true hydraulic fractures outline a remarkably uniform orientation for the maximum horizontal principal stress direction, namely N 155±10°E.

This has prompted Gunzburger and Magnenet (2014) to propose an elastic model for this stress field, assuming an "Alpine push" hypothesis as the source of present-day stresses.

Indeed, the present-day deformation rate is beyond direct observation according to Nocquet (2012): velocities linked to present-day deformation are smaller than 1 mm/y. This has led Gunzburger and Magnenet to consider that the present-day stress field results from the long term elastic response of the region following the last tectonic phase, namely the final "Alpine" activity, some 5 million years ago. Isotropic elastic moduli have been determined for the various layers so as to fit Wileveau et al.'s observed vertical stress profiles.

But Gonçalves et al. (2004) investigated the pore pressure variations generated by a poro-elastic response of the argillite layer because of an Alpine push. They concluded that the overpressure in the argillite should have dissipated within the half million years following the end of the tectonic activity. Hence, elastic modelling leaves unexplained the present-day pore pressure profile in the argillite.

In addition, laboratory work on the mechanical behavior of the argillite (Zhang and Rothfuchs, 2004) has shown that the argillite exhibits a Burger type visco-elastic behavior (long term fluid behavior). According to this observation, the shear stress component supported by the argilite because of the "Alpine push", should have relaxed completely by now.

Hence because of both the present-day shear stress and the pore pressure profile observed in the argillite, we conclude that a purely elastic model associated with an "Alpine push" leaves unanswered two key features of the argillite hydro-mechanical behavior.

In addition, vertical seismic profiles that have been conducted in 2000 m deep wells, some 100 km to the west of the Bure site, have outlined an orthotropic elastic behavior for both the Dogger and the Oxfordian limestones (Lefeuvre et al., 1992). Interestingly, detailed mapping of natural fractures in the various formations has outlined a significant density of vertical fractures oriented N155° E in both the Oxfordian and the Dogger limestones (André et al., 2006).

Hence the elastic orthotropy of the materials is generated by the combination of sub-horizontal beds together with the vertical fractures field preferentially oriented N 155°E.

We conclude that gravity alone acting on this orthotropic sedimentary material may be the unique source of present day stresses. But this leaves unanswered the two questions concerning the pore pressure and the shear stress in the fluid-type visco-elastic argillite.

4.2. A new visco-poro-elastic model

In their attempt at modeling the vertical stress profiles observed at Bure, *Günzburger and Magnet* (2014) noticed that best fitting elastic parameters identified for the limestones were much lower than values computed from elastic waves propagation data derived from sonic logs. They concluded on the existence of a long term softening process affecting the limestone behavior, which they proposed to link to pressure solution effects.

Natural fracture constitutes a privileged site for the development of pressure solution (Yasuhara and Elsworth, 2004; Renard et al. 2012). Micro-displacements are generated in the direction normal to the fracture planes. Hence, for a large fractured rock volume, pressure solution generates a rock volume decrease, the geometry of which depends on the fracture field morphology.

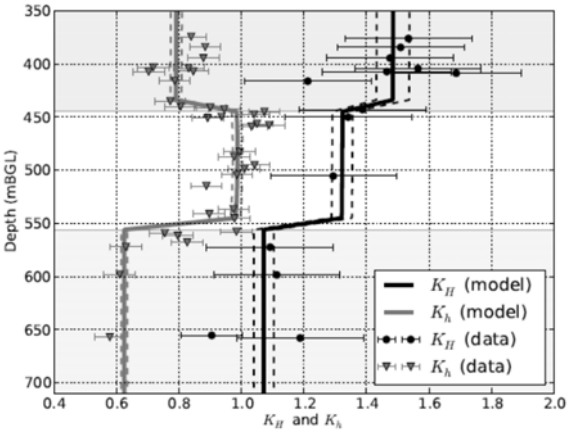

Fig. 6. Comparison between measured (dots with error bars) and computed values (continuous lines). Only the ratios $K_H = \sigma_H/\sigma_v$ and $K_h = \sigma_h/\sigma_v$ are plotted. The dotted lines on both sides of the continuous curves correspond to ± 10% variations of relevant elastic moduli.

This observation has led Magnenet et al. (2017) to propose a simple hydromechanical model characterized by two main features linked to pressure solution effects. The first one (equation 8) concerns a time-dependent orthotropic mechanical behavior associated with pressure solution in fractures. The second one (equation 9) introduces a coupling term in the fluid mass balance equation involving volumetric strain because of the mass transfer from the solid to the fluid:

$$\mathbf{C(t)= C^{iso}} + t/\tau_{ps}\ (C^{ort}- C^{iso}) \quad 0 < \tau < \tau_{ps} \qquad (8)$$

$$\partial\, m_f / \partial\, t + \nabla .\, M_f = \beta \qquad (9)$$

C(t) is the orthotropic compliance matrix at time t, whilst the asymptotic value, as time passes, is C^{ort}. For t = 0, the material is assumed to be isotropic (C^{iso}).

In closed systems, pressure solution stops when the ion concentration in the fluid near asperities gets smaller than a critical value that depends on local conditions (Yasuhara and Elsworth, 2004). Hence τ_{ps} depends on

these local conditions. It is considered to lie in the range 10^4 to 10^5 years.

In the fluid mass balance equation (9), the term β describes the rate of solid dissolution into the fluid. It also depends on local conditions.

Equations (8) and (9) have been implemented in a one D model with gravity loading only, i.e; assuming no displacement in the horizontal direction and a Darcy law for the fluid flow. The model parameters have been inverted with a least squares algorithm so as to fit stress and pore pressure observations (figures 6 and 7).

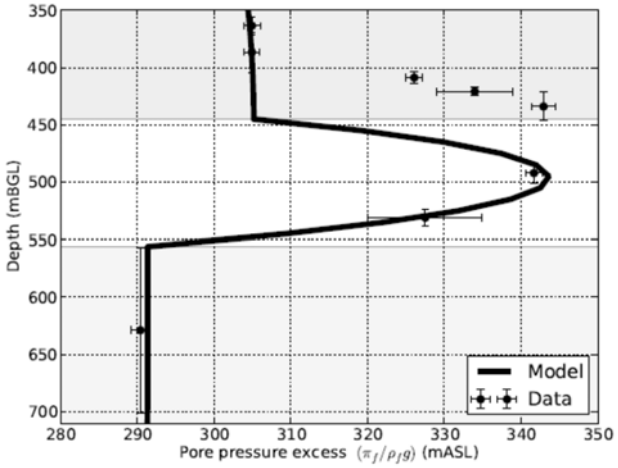

Fig. 7. Pore pressure profile near the underground laboratory

4.3. Influence of climate change on the present day stress field

The model developed by Magnenet et al. assumes an arbitrary value of 1000 years for τ_{ps} for their objective is only to test the physical consequences of pressure solution, not to concentrate on real time constant. The important conclusion is that this effect alone stops after a certain time and therefore cannot explain the present day stress and pore pressure in the argillite.

But recent studies (Jost et al. 2007), have shown that climatic variations have influenced the local pore pressure down to the argillite, in the Paris Basin. Indeed, because of permafrost development during the last glaciation, meteoritic water stopped percolating through the upper permeable layers. But the disappearance of permafrost some 13000 years ago has let the meteoritic water percolation to resume. This resulted in some pressure gradient that induced some deep fluid motion down to the argillite. This perturbed ions concentrations near asperities in fractures so that pressure solution has been reactivated within the last 10 000 years. Such fluid motion variations occur with all glaciation cycles.

5. CONCLUSION A NEW PARADIGM FOR INTRAPLATE STRESS FIELDS

We may conclude that the present-day stresses and pore-pressure profiles in the argillite imply a present day deformation, when no such present day deformation can be detected by continuous GPS monitoring. This implies some endogenous mechanism which cannot be linked to far field geodynamic conditions.

This observation is corroborated by an examination of the micro-seismic map of France (Fig. 8)

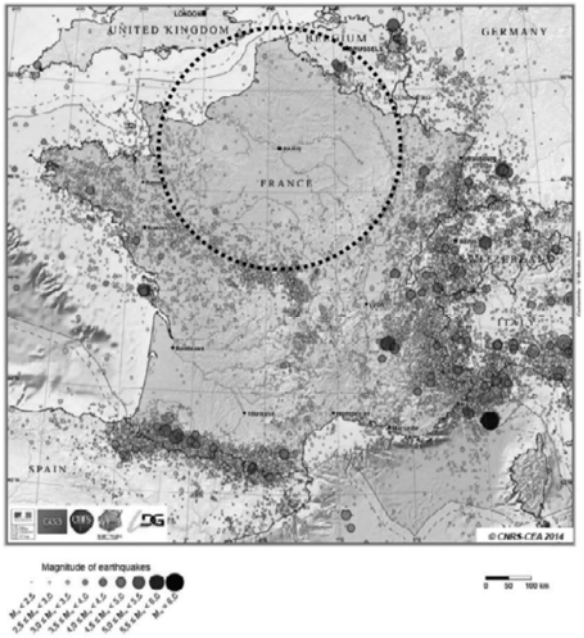

Fig. 8. Map of France micro-seismicity. The Paris Basin is outlined by the doted circle.

No seismic activity is observed in the Paris Basin but some micro-seismicity is observed all around. The far field geodynamic conditions are the same for both locations, which demonstrates that the source of micro-seismicity depends only on local conditions.

Interestingly micro-seismicity is observed in old mountainous massifs, where meteoritic water may percolate quite deep, but it is absent in locations where impervious formations prevent this deep fluid circulation.

It is proposed that the regional stress field in the upper kilometers of intraplate regions is controlled by gravity alone, by the local materials rheology, and by fluid circulations.

ACKNOWLEDGEMENTS

I thank very sincerely S. Glaser and P. Smealie for inviting me to give this MTS lecture. Many of the discussed results have been sponsored by ANDRA.

REFERENCES

1. André, G., B. Proudhon, H. Rebours, and Y. Willeveau. 2006. Paramètres contrôlant la distribution de la fracturation : exemple dans une série marno-calcaire du Jurassique. *C.R. Geoscience* ; 338, 931-941.
2. Berard, T., and F.H. Cornet. 2003. Evidence of thermally induced borehole elongation: a case study at Soultz, France. *Int. J. Rock Mech. Min. Sc*., 40, 1121-1140.
3. Cornet, F.H. 1993. The HTPF and the Integrated stress determination methods. In *Comprehensive Rock Engineering* (Hudson ed.); Vol 3, ch. 15, pp 413-432 Pergammon Press, Oxford
4. Cornet, F.H. 2015. *Elements of crustal Geomechanics*, 460 p., Cambridge University press.
5. Cornet, F.H., and B. Valette. 1984. In-situ Stress Determination from Hydraulic Injection Test Data; *J. Geoph. Res*.; 89(B13), 11,527 – 11,537.
6. Cornet, F.H., and J.M. Yin. 1995. Analysis of induced seismicity for stress field determination and pore pressure mapping. *Pure App. Geophys*., 145, 677-700.
7. Cornet, F.H., M.M. Doan, and F. Fontbonne. 2003. Electrical imaging and hydraulic testing for a complete stress determination. *Int. J. Rock mech. Min. Sc.,* 40, 1225-1241.
8. Cornet F.H. and T. Roeckel. 2012. Vertical Stress profiles and the significance of stress decoupling; *Tectonophysics*; 581, 193-205.
9. Delay, J., M. Distinguin, and S. Dewonck. 2007. Characterization of a clay-rich rock through development and installation of specific hydrogeological and diffusion test equipment in deep boreholes. *Phys. Chem. Earth;* 32, 293-407.
10. Gephart, J.W., and D.W. Foryth. 1984. An improved method for determining the regional stress tensor using earthquale focal mechanisms data: application to the San Fernando earthquake sequence; *J. Geophys. Res.,* 89, 9305-9320
11. Gonçalves, J, S. Violette, and J. Wendling. 2004. Analytical and numerical solutions for alternative overpressuring processes: Application to the Callovo-Oxfordian sedimentary sequence in the Paris Basin, France. *J. Geophys. Res.,* 109, B02,110.
12. Gunzburger, Y., and V. Magnenet. 2014. Stress inversion and basement-cover stress transmission across weel layers in the Paris Basin, France. *Tertonophysics*, 617, 44-57.
13. Haimson, B.C., and F.H. Cornet. 2003. ISRM suggested methods for rock stress estimation-Part 3: hydraulic fracturing (HF) and /or hydraulic testing of pre-existing fractures (HTPF*). Int. J. Rock Mech. Min. Sc*., 40, 1011-1050.
14. Heidbach, O., M. Tingay, A. Barth, J. Reinecker, D. Kurfess, and B. Müller. 2010. *Tectonophysics*, 482, 3-15.
15. Ito, T., K. Evans, K. Kawai, and K. Hayashi. 1999. Hydraulic fracture reopening pressure and the estimation of the maximum horizontal principal stress. *Int. J. Rock Mech. Min. Sc*., 36, 811-826.
16. Lefeuvre, F., L. Nikoletis, V. Ansel, and C. Cliet. 1992. Detection and measure of birefringence from vertical seismic data: theory and application. *Geophysics,* 57, 1463-1481.
17. Lei, T., B.K. Sinha, and M. Sanders. 2012. Estimation of horizontal stress magnitudes and stress coefficients of velocities using borehole sonic data. *Geophysics*, 77, WA181-WA196.
18. Magnenet, V., F.H. Cornet, and C. Fond. 2017. A non-tectonic origin for the present-day stress filed in the Paris Basin. Submitted to *J. Geophys. Res.*
19. Maury, J., F.H. Cornet, and L. Dorbath. 2013. A review of methods for determining stress fields from focal mechanisms: application to the Sierentz 1980 seismic crisis (Upper Rhine Grabben); *Bull. Soc. Geol. Fr*., 184, 319-334.
20. Nocquet, J.M., 2012. Present-day kinematics of the Mediterranean: a comprehensive overview of GPS results. *Tectonophysics*, 579, 220-242.
21. Pesca, P., and M.D. Zoback. 1995. Compressive and tensile failure of inclined well bores and determination of *in situ* stress and rock strength. *J. Geophys. Res.,* 100; 12,791-12,811.
22. Renard F., K. Mair, and O. Gundersen. 2012. Surface roughness evolution on experimentally simulated faults. *J. Struct.Geol*., 45, 101-112
23. Wileveau, Y., F.H. Cornet, J. Desroche, and P. Blumling. 2007. Complete in situ stress determination in an argillite sedimentary formation *Phys. Chem. Earth*, 32, 866-878
24. Yasuhara, H., and D. Elsworth. 2004. Evolution of permeability in a natural fracture: significant role of pressure solution. *J. Geophy. Res*.; 109, B03,304.
25. Yin, J.M., and F.H. Cornet. 1994. Integrated stress determination by joint inversion of hydraulic tests and focal mechanisms. *Geophys. Res. Lett*., 21, 2645-2648.
26. Zhang, C., and T. Rothfuchs. 2004. Experimental study of the hydromechanical behavior of the Callovo-Oxfordian argillite. *App. clay Sc.,* 26, 325-336.
27. Zoback, M.L. 1992. First- and second-order patterns of stress in the Lithosphere: The world stress map project *J. Geophys. Res.* 97 (B8): 11,703–11,728.
28. Zoback, M.D. 2007. *Reservoir Geomechanicss*, 450 p., Cambridge University Press.